Asymmetric seasonal temperature trends

Judah L. Cohen[1], Jason C. Furtado[1], Mathew Barlow[2], Vladimir A. Alexeev[3] and Jessica E. Cherry[3]

[1]Atmospheric and Environmental Research, Lexington, Massachusetts 02421, USA.

[2]Environmental, Earth, and Atmospheric Sciences, University of Massachusetts Lowell, Massachusetts 01854, USA.

[3]International Arctic Research Center, University of Alaska Fairbanks, Fairbanks, AK 99775, USA.

Current consensus on global climate change predicts warming trends driven by anthropogenic forcing, with maximum temperature changes projected in the Northern Hemisphere (NH) high latitudes during winter. Yet, global temperature trends show little warming over the most recent decade or so. For longer time periods appropriate to the assessment of trends, however, global temperatures have experienced significant warming for all seasons except winter, when cooling trends exist instead across large stretches of eastern North America and northern Eurasia. Hence, the most recent lapse in global warming is a seasonal phenomenon, prevalent only in boreal winter. Additionally, we show that the largest regional contributor to global temperature trends over the past two decades is land surface temperature in the NH extratropics. Therefore, proposed mechanisms explaining the

fluctuations in global annual temperature trends should address this apparent seasonal asymmetry.

1. Introduction

Global surface temperatures are projected to warm due to rapid increases in greenhouse gases (GHGs) and over the entire length of the instrumental record, temperatures have undergone a warming trend [*IPCC*, 2007]. However it has been noted that the global warming trend has slowed and even halted since the late 1990s [e.g., *Easterling and Wehner,* 2009; *Kaufmann et al.,* 2011]. Several studies have offered explanations for the recent cessation in the global temperature trend, including climate variations of the North Atlantic and equatorial Pacific oceans [*Keenlyside et al.,* 2008; *Meehl et al.,* 2011], variations in solar activity [*Lean and Rind,* 2009], changes in stratospheric water vapor [*Solomon et al.,* 2010], and tropospheric aerosols [*Kaufmann et al.,* 2011]. The sudden absence of a warming trend is not particularly unique or even unexpected. Easterling and Wehner [2009], through running decadal trend analysis, show that even the observed record has decadal spans of little to no warming. Even coupled climate model simulations of a future warmer world due to increased GHGs contain periods of little to no warming [*Easterling and Wehner,* 2009; *Meehl et al.,* 2011]. Indeed, large-scale modes of natural variability in the atmosphere and ocean may work to negate radiative warming on decadal timescales.

The aforementioned studies discuss the absence of a warming trend or even a cooling trend in the context of global annual temperatures. Yet, analysis of temperature trends

seasonally is not extensively reported, both in the observational record and in coupled climate model simulations. As we will illustrate, recent trends in global surface temperatures are seasonally-dependent; i.e., only Northern Hemisphere (NH) extratropical land surface temperatures during boreal winter display a systematic waning of the warming trend to a near-neutral trend of late. The implications of this finding are important for testing the relative importance of the proposed mechanisms suggested for the cessation of the warming trend and for evaluating how coupled climate models can handle such seasonal asymmetries.

2. Observational Data and Model Output

Observational surface temperature data originate from two sources: (1) The Climate Research Unit land air temperature dataset, version 3 [CRUTEM3; *Brohan et al.,* 2006]; and (2) The National Aeronautics and Space Administration Modern Era Retrospective-Analysis for Research and Applications [NASA MERRA; *Rienecker et al.,* 2011]. The CRUTEM3 dataset, consisting of monthly land station-based temperature anomalies, are on a regular 5° x 5° longitude/latitude grid globally. The data are provided as anomalies, using the 1961-1990 period as the base period, and extend from 1850 to present. NASA MERRA monthly-mean surface temperatures reside on a 1.25° x 1.25° grid globally, covering land and ocean, starting from 1979 to present. Monthly-mean anomalies from MERRA are computed by removing the climatological monthly means (1979-2011) from the raw data.

Coupled-climate model output are provided from the Coupled Model Intercomparison

Project Phase 5 (CMIP5) multi-model ensemble archive, available for download from the Program for Climate Model Diagnosis and Intercomparison (PCMDI) at the Lawrence Livermore National Laboratory (more information on the program is provided online at **http://cmip-pcmdi.llnl.gov/cmip5/**). We used all available ensemble members of the decadal1980 scenario (i.e., the model runs are initialized with conditions as in 1980 and run for 30 years using mainly observed natural and anthropogenic forcing). Six models were available and analyzed for this study (see Table 1), each with multiple realizations. Surface temperature output from the models is interpolated from their native model grids to a common 2.5° by 2.5° longitude/latitude grid for comparison. Surface temperature anomalies are then computed by removing the climatological monthly mean from 1980-2010. Model results are shown as the ensemble-mean of all models and all realizations.

When examining seasonal temperature trends, seasons are defined as follows: December – February (DJF) as boreal winter, March – May (MAM) as boreal spring, June – August (JJA) as boreal summer, and September – November (SON) as boreal fall. To test the robustness of any trends, given that the period 1999-2010 spans twelve years, we computed and tested the significance of multiple periods divisible by six. Therefore we also computed the temperature trend for the following periods: 2005-2010, 1999-2010, 1993-2010 and 1987-2010. For completeness, we also computed the trend and significance for the longer period 1979-2010, which includes the full period that satellite data is assimilated into the reanalysis datasets [*Kalnay et al.,* 1996]. Trends for all periods are shown in degrees Celsius per five years for comparative purposes.

3. Results and Discussion

Figure 1 presents the linear temperature changes from the CRUTEM3 dataset over five periods (1979-2010, 1987-2010, 1993-2010, 1998-2010, and 2005-2010) and four regions: globally (Fig. 1a), the NH extratropics (20-90°N; Fig. 1b), the tropics (20°N-20°S; Fig. 1c) and the Southern Hemisphere (SH) extratropics (20°-90°S; Fig. 1d). Examining the annual temperature trends, we find that the rate of global temperature increase has diminished when looking at more recent periods, and this phenomenon is seen outside of the tropics. Indeed, only the tropics display a significant warming trend for the 1999-2010 interval (Fig. 1c) – elsewhere the trends are not significantly different from zero. The NH extratropics contains large trends (Fig. 1b), as expected from examining land surface records, while the SH extratropical landmasses have much smaller trends (Fig. 1d).

Upon examining temperature trends seasonally, the global temperature record reveals that significant warming occurs in three seasons (boreal spring, summer, and fall) for the four earliest periods (i.e., 1979-2010, 1987-2010, 1993-2010, and 1999-2010). However, boreal winter (DJF) is the glaring exception in the record – only when starting from 1979-2010 is the DJF warming significant. For the following periods, the trend is no longer significant and even turns negative over the last decade. The only sub-region that mirrors this behavior in global temperature trends is the NH extratropics (Fig. 1b).

To check the robustness of this seasonal asymmetry and also examine potential influences of ocean temperatures on the global temperature trend, we repeat the analysis from Fig. 1 but using NASA MERRA surface temperature data (Fig. 2). Inclusion of sea surface temperatures (SSTs) with land temperatures yields similar trend results as from the

land-only CRUTEM3 data – i.e., insignificant winter warming trends since the 1980s despite significant warming in the other seasons (Fig. 2a). Global linear temperature trends are also dominated by the trends in the NH extratropics (Figs. 2b and 2e). When examining changes in the trend in NH land and ocean temperatures, we find that SSTs exhibit robust, significant warming annually and seasonally as late as a start in 1993 (Fig. 2e). Land regions show similar robust warming annually and for all seasons but winter, the only season with no statistically significant warming for any period (Fig. 2b). The tropics have no significant trends in land temperatures or SSTs except when going back to 1979 (Figs. 2c and 2f), and trends in the SH ocean and land are somewhat more random and even inconsistent between MERRA and the CRUTEM3 datasets (Figs. 2d and 2g; differences are likely a function of different sampling). Staggering start and end dates by 1-2 years yields similar results for both NASA MERRA and CRUTEM3 (not shown). Hence, we confidently conclude that the cessation of global winter warming since 1987 is mostly attributable to neutral or even cooling temperature trends across the NH extratropical landmasses. We further computed the same trends using an observational ocean dataset [*Smith et al.,* 2008 (shown in Supplementary Fig. S1)] and ERA-Interim [*Dee et al.*, 2011 (not shown)] and though trends differ slightly by region, the absence of winter warming is still tied to NH extratropical land cooling.

Focusing on the NH extratropical land surface temperature trends since 1987, Figure 3 shows both the area-averaged temperature anomaly seasonally (Fig. 3a) and spatially (Figs. 3b-3e). Rapid and significant warming is clearly evident in all seasons but winter, with the boreal fall land surface temperatures warming the most rapidly. For DJF, the linear temperature trend is nearly zero. Of importance is the spatial pattern of the linear

124 temperature trends (Figs. 3b-3e). For boreal summer and fall, except for select areas, most
125 of the NH landmasses are experiencing strong warming trends, at or exceeding 1°C per
126 decade in central and northern Eurasia (Figs. 3d and 3e). Except for pronounced cooling in
127 western and northwestern North America, boreal spring temperatures also are warming
128 strongly (Fig. 3c). However, corresponding to the near-neutral wintertime trend are large
129 regions of significantly strong cooling trends across Europe, northern and central Asia, and
130 parts of central and eastern North America (Fig. 3b). This spatial pattern of temperature
131 trends is reminiscent of the temperature regression pattern associated with the negative
132 phase of the Arctic Oscillation [AO; e.g., *Thompson and Wallace,* 2001]. Indeed, the
133 pattern correlation between the winter temperature trend pattern and the temperature
134 anomaly pattern associated with the negative phase of the AO is 0.85 ($p < 0.01$).

135 The absence of a warming trend in winter is especially surprising given that coupled
136 climate models project the strongest warming across the NH during boreal winter due to
137 'winter (or Arctic, polar) amplification' [*Holland and Bitz,* 2003; *Alexeev et al.,* 2005;
138 *Langen and Alexeev,* 2007; *Serreze and Barry,* 2011]. We computed the seasonal
139 temperature trends and anomalies from the decadal1980 runs available from the CMIP5
140 model archive for the period 1987-2010. Independent of region or season, the models
141 forecast positive temperature trends throughout all time periods, with insignificant warming
142 only over the 2000s (see Supplementary Fig. S2). The model simulated interannual
143 seasonal temperatures are compared with the NASA MERRA seasonal temperature
144 anomalies in Figure 4. The annual ensemble-mean NH extratropical land surface
145 temperatures (solid black line in Fig. 4a) track well with the observed annual NH

146 extratropical land surface temperatures (red line in Fig. 4a), though the ensemble-mean
147 slightly underestimates the total linear trend for the period ($\Delta T_{ENSMEAN}$ = 0.32°C versus
148 ΔT_{OBS} = 0.49°C). For a more complete comparison of the observed temperatures with the
149 model simulated temperatures we include a spaghetti plot of all ensemble members in
150 Figure S3.

151 The models also simulate closely the seasonal trends for spring, summer and fall. For
152 winter, while there is much more interannual variability in the observed versus simulated
153 temperatures (the observed temperature falls outside the 1σ envelope two thirds of the time,
154 double what is expected), the correspondence between DJF observed and simulated
155 temperature trends remains the weakest of the four. Clearly, the difference in the boreal
156 winter temperature trends represents some poorly resolved or missing forcing that is less
157 influential in the other three seasons. We also note that the models predict robust cooling
158 in all seasons due to the radiative forcing from the volcanic eruption of Mount Pinatubo.
159 The simulated cooling is similar to the observations in all seasons except winter. This
160 suggests that radiative forcing important in spring, summer and fall is likely masked by
161 dynamic forcing associated with wave driving in winter. Ongoing research suggests that the
162 models are deficient in simulating fall snow cover variability and wave forced stratosphere-
163 troposphere coupling, which is contributing to poor model simulations of the AO and NH
164 winter climate trends [e.g. *Hardiman et al.,* 2008; *Cohen et al.,* 2012]. As the leading mode
165 of NH wintertime climate variability, differences in the observed versus simulated AO are
166 likely an important factor. Indeed, when examining the evolution of the AO and associated
167 sea level pressure trends across the NH, we find a divergence in the observed trends – the

observations illustrate a trend toward *negative* AO conditions during DJF, while the models actually suggest a slight *positive* trend in the index (Supplementary Fig. S4a). Spatially, observations indicate statistically significant positive trends in sea level pressure (SLP) at high latitudes with statistically significant negative trends in SLP at lower latitudes (i.e., a negative AO pattern), while the models predict no significant SLP trends over the period.

4. Summary and Conclusions

Analysis of monthly and annual temperatures over the past decade shows that the positive global temperature trend has become insignificant and small. Based on previously reported analysis of the observations and modelling studies this is neither inconsistent with a warming planet nor unexpected; and computation of global temperature trends over longer periods does exhibit statistically significant warming. However, upon examining the trends seasonally, more interesting and significant findings are discovered. In examining the NH extratropical landmasses, the biggest contributor to global temperature trends, we find substantial divergence in trends between boreal winter and the other three seasons. A statistically significant warming trend is *absent* across NH landmasses during DJF going back to at least 1987, with either wintertime near-neutral or cooling trends. In contrast, significant warming is found for the other three seasons over the same time period.

Based on current literature and our own examination of the latest coupled climate models, the lack of a significant warming trend in winter spanning nearly three decades is not likely or expected (less than 10% of the ensemble members analyzed in this study predicted no warming in winter). Therefore, we argue that any attribution study on the recent cessation of global warming should explicitly explain the seasonally asymmetric

nature of the temperature trend. For example, studies that attribute the recent cooling to diminished shortwave radiation at the surface are at a great disadvantage since their influence is maximized during boreal summer and minimized during boreal winter, opposite to what has been observed.

There are theories that argue for recent cooling that is limited to the winter season. One theory is known as 'warm Arctic cold continents,' where a warmer Arctic and declining Arctic sea ice are contributing to colder winters across the NH continents [*Honda et al.* 2009; *Budikova*, 2009; *Francis et al.,* 2009; *Overland and Wang,* 2010; *Petoukhov and Semenov,* 2010; *Serreze et al*., 2011]. A second theory is that increasing fall Eurasian snow cover that may also be related to a warming Arctic is forcing a negative trend in the winter AO [*Cohen and Barlow,* 2005; *Cohen et al.,* 2009; *Cohen et al.,* 2012]. As Figure 3b illustrates, the observed winter temperature trend spatially resembles the pattern of temperatures associated with the negative phase of the AO. Therefore, the inability of the models to simulate the observed trend in the AO (Fig. S4), may partly explain the poorly simulated DJF temperature trends.

Acknowledgements. JLC is supported by the National Science Foundation grants ARC-0909459 and ARC-0909457 and NOAA grant NA10OAR4310163. VA and JEC were supported by the National Science Foundation grants ARC 0909525 and Japan Agency for Marine-Earth Science and Technology. The authors acknowledge the climate modelling groups (listed in table S1 of this paper), the World Climate Research Programme's (WCRP) Working Group on Coupled Modelling (WGCM), and the Global Organization for Earth System Science Portals (GO-ESSP) for producing and making the CMIP5 model simulations available for analysis.

References

217 Alexeev, V. A., P. L. Langen, and J. R. Bates (2005), Polar amplification of surface
218 warming on an aquaplanet in "ghost forcing" experiments without sea ice
219 feedbacks, *Climate Dynamics*, 24 (7-8), 655-666, doi: 10.1007/s00382-005-0018-3.
220 Brohan, P., J. J. Kennedy, I. Harris, S. F. B. Tett, and P. D. Jones (2006), Uncertainty
221 estimates in regional and global observed temperature changes: A new dataset from
222 1850, *J. Geophys. Res.*, *111,* D12106, doi:10.1029/2005JD006548.
223 Budikova, D. (2009), Role of Arctic sea ice in global atmospheric circulation: A review.
224 *Global Planet. Change, 68(3),* 149–163.
225 Cohen, J., and M. Barlow (2005), The NAO, the AO, and global warming: How closely
226 related? *J. Climate, 18*, 4498–4513, doi: 10.1175/JCLI3530.1.
227 Cohen, J., M. Barlow, and K. Saito (2009), Decadal fluctuations in planetary wave forcing
228 modulate global warming in late boreal winter, *J. Climate, 22*, 4418–4426, doi:
229 10.1175/2009JCLI2931.1.
230 Cohen, J., J. C. Furtado, M. A. Barlow, V. A. Alexeev and J. E. Cherry (2012) Arctic
231 warming, increasing fall snow cover and widespread boreal winter cooling,
232 *Environ. Res. Lett.*, 7, 014007 doi:10.1088/1748-9326/7/1/014007.
233 Dee, D. P., and Co-Authors (2011), The ERA-Interim reanalysis: configuration and
234 performance of the data assimilation system, *Quart. J. R. Meteorol. Soc.*, *137*, 553-
235 597.
236 Easterling, D. R., and M. F. Wehner (2009), Is the climate warming or cooling?, *Geophys.*
237 *Res. Lett.*, 36, L08706, doi:10.1029/2009GL037810.

238 Francis, J. A., W. Chan, D. J. Leathers, J. R. Miller, and D. E. Veron (2009), Winter
239 Northern Hemisphere weather patterns remember summer Arctic sea-ice extent,
240 *Geophys. Res. Lett., 36*, L07503, doi:10.1029/2009GL037274.
241 Hardiman, S. C., P. J. Kushner, and J. Cohen (2008) Investigating the ability of general
242 circulation models to capture the effects of Eurasian snow cover on winter climate,
243 *J. Geophys. Res., 113*, D21123, doi:10.1029/2008JD010623.
244 Holland, M. M. and C. M. Bitz (2003), Polar amplification of climate change in coupled
245 models, *Climate Dynamics, 21*, 221–232.
246 Honda, M., J. Inoue, and S. Yamane (2009), Influence of low Arctic sea-ice minima on
247 anomalously cold Eurasian winters, *Geophys. Res. Lett.*, *36*, L08707,
248 doi:10.1029/2008GL037079.
249 IPCC (2007), *Climate Change 2007: The Physical Science Basis. Contribution of Working*
250 *Group I to the Fourth Assessment Report of the Intergovernmental Panel on*
251 *Climate Change* [Solomon, S., D. Qin, M. Manning, Z. Chen, M. Marquis, K. B.
252 Averyt, M. Tignor and H. L. Miller (eds.)]. Cambridge University Press,
253 Cambridge, United Kingdom and New York, NY, USA, 996 pp.
254 Kalnay, E., M. Kanamitsu, R. Kistler, W. Collins, D. Deaven, L. Gandin, M. Iredell, S.
255 Saha, G. White, J. Woollen, Y. Zhu, M. Chelliah, W. Ebisuzaki, W. Higgins, J.
256 Janowiak, K. C. Mo, C. Ropelewski, J. Wang, A. Leetmaa, R. Reynolds, R. Jenne,
257 and D. Joseph (1996), The NCEP/NCAR 40-Year reanalysis project, *Bull. Amer.*
258 *Meteor. Soc.*, *77*, 437-471, doi: 10.1175/1520-
259 0477(1996)077<0437:TNYRP>2.0.CO;2.
260 Kaufmann, R. K., H. Kauppi, M. L. Mann, and J. H. Stock, (2011), Reconciling

anthropogenic climate change with observed temperature 1998–2008, *Proc. Nat. Acad. Sci*., doi: 10.1073/pnas.1102467108.

Langen, P. L., and V. A. Alexeev (2007), Polar amplification as a preferred response in an aquaplanet GCM, *Climate Dynamics*, *29*(2-3), 305-317, doi:10.1007/s00382-006-0221-x.

Lean, J. L., and D. H. Rind (2009), How will Earth's surface temperature change in future decades? *Geophys. Res. Lett.*, *36*, L15708, doi:10.1029/2009GL038932.

Keenlyside, N. S., M. Latif, J. Jungclaus, L. Kornblueh, and E. Roeckner (2008), Advancing decadal-scale climate prediction in the North Atlantic sector, *Nature*, *453*(84-88), doi:10.1038/nature06921.

Meehl, G. A., J. M. Arblaster, J. T. Fasullo, A. Hu, and K. E. Trenberth (2011), Model-based evidence of deep-ocean heat uptake during surface-temperature hiatus periods, *Nature Climate Change*, doi:10.1038/nclimate1229.

Overland, J. E., and M. Wang (2010), Large-scale atmospheric circulation changes are associated with the recent loss of Arctic sea ice, *Tellus, 62A*, 1-9.

Petoukhov, V., and V. A. Semenov (2010), A link between reduced Barents-Kara sea ice and cold winter extremes over northern continents, *J. Geophys. Res*., *115*, D21111, doi:10.1029/2009JD013568.

Rienecker, M. M. *et al.* (2011), MERRA - NASA's Modern-Era Retrospective Analysis for Research and Applications, *J. Climate, 24,* 3624-3648, doi: 10.1175/JCLI-D-11-00015.1.

Serreze, M. C. and R. G. Barry (2011), Processes and impacts of Arctic amplification: A research synthesis, *Global and Planetary Change*, *77*, 85–96.

284 Serreze, M. C., A. P. Barrett, and J. J. Cassano (2011), Circulation and surface controls on
285 the lower tropospheric air temperature field of the Arctic, *J. Geophys. Res.*, *116*,
286 D07104, doi:10.1029/2010JD015127.
287 Smith, T. M, R. W. Reynolds, T. C. Peterson, and J. Lawrimore (2008), Improvements to
288 NOAA's historical Merged Land-Ocean Surface Temperature Analysis (1880-
289 2006), *J. Climate*, *21*, 2283-2296.
290 Solomon, S., K. H. Rosenlof, R. W. Portmann, J. S. Daniel, S. M. Davis, T. J. Sanford, and
291 G.-K. Plattner (2010), Contributions of Stratospheric Water Vapor to Decadal
292 Changes in the Rate of Global Warming, *Science*, 327, 1219-1223,
293 doi:10.1126/science.1182488.
294 Thompson, D. W. J., and J. M. Wallace (2001), Regional climate impacts of the Northern
295 Hemisphere Annular Mode, *Science*, *293*, 85–89.
296

296 **Figure Legends**

297 **FIG. 1.** (a) The linear trend in area-averaged global land surface temperature (°C per 5
298 years) determined from CRUTEM3 for five different periods: 1979-2010 (dark red), 1987-
299 2010 (light blue), 1993-2010 (green), 1999-2010 (orange), and 2005-2010 (pink). Filled
300 bars represent trends that are significant at the 95% significance level. (b) As in (a) but
301 only for the NH (20°N-90°N). (c) As in (a) but for the tropics (20°N-20°S). (d) As in (a)
302 but for the Southern Hemisphere (SH; 20°S-90°S).

303

304 **FIG. 2.** (a) The linear trend in area-averaged global surface temperature (°C per 5 years)
305 over *land and ocean* from the NASA MERRA dataset. Filled bars represent trends that are
306 significant at the 95% significance level. (b)-(d) The linear trend in averaged *land* surface
307 temperature only (°C per 5 years) in the (b) NH (20°N-90°N), (c) tropics (20°N-20°S), and
308 (d) SH (20°S-90°S). Filled bars as in (a). (e)-(g) As in (b)-(d) but for *ocean* surface
309 temperatures.

310

311 **FIG. 3. (**a) Surface temperature anomalies (solid lines; °C) from CRUTEM3 averaged
312 poleward of 20°N from 1988 – 2010 for the four seasons: winter (DJF), spring (MAM),
313 summer (JJA), and fall (SON). Linear trend lines (dashed lines) superimposed for each
314 season, with the magnitude of the trend (°C per 10 years) and statistical significance shown.
315 The spatial pattern of linear trends in surface temperature (°C per 10 years) are shown for:
316 b) winter, c) spring, d) summer and e) fall.

317

318 **FIG. 4.** (a) (red line) Annual land surface temperature anomaly (°C), area-averaged
319 poleward of 20°N, from NASA MERRA from 1987-2010. (black line) The CMIP5
320 ensemble-mean annual land surface anomaly, area-averaged poleward of 20°N. Gray
321 shading represents ±1σ from the ensemble-mean. (b)-(e) As in (a) but for (b) DJF, (c)
322 MAM, (d) JJA, and (e) SON-averaged NH land surface temperature anomaly.
323
324
325
326
327
328
329
330
331
332
333
334

334 **Table 1.** The six coupled climate models from the CMIP5 model archive analyzed for this study. Number of
335 ensemble members for the decadal1980 scenario is also indicated.

Modelling Agency, Country	Model Name	Ensemble Members
Canadian Climate Centre for Modelling and Analysis, Canada	CanCM4	10
Météo-France/Centre National de Recherches Météorologiques, France	CNRM-CM5	10
Hadley Centre for Climate Prediction and Research/Met Office, United Kingdom	HadCM3	10
Center for Climate System Research, Japan	MIROC4h	3
Center for Climate System Research, Japan	MIROC5	6
Meteorological Research Institute, Japan	MRI-CGCM3	3

336

337

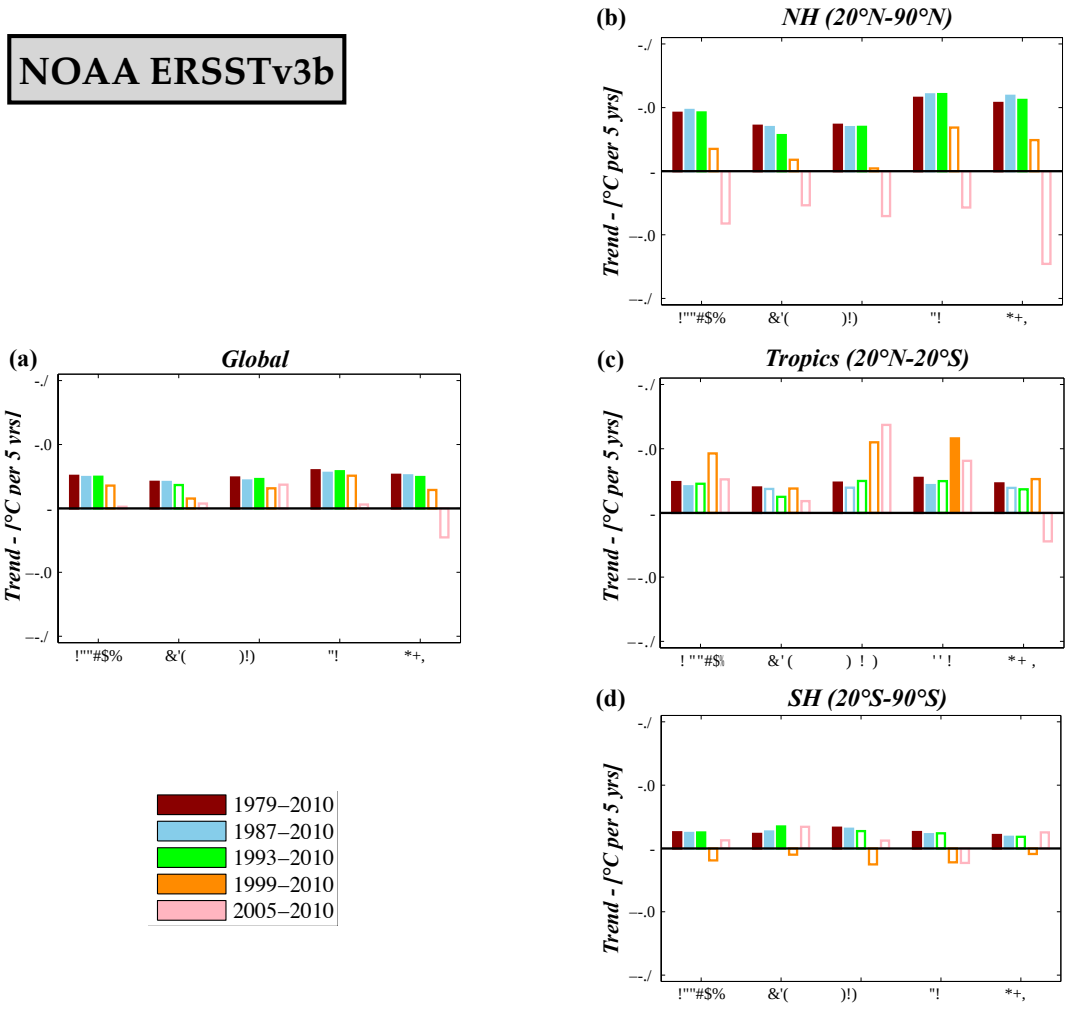

Fig. S1. (a) The linear trend in °C per 5 years area-averaged global ocean surface temperature (°C), determined from NOAA ERSSTv3b for five different periods: 1979-2010 (dark red), 1987-2010 (light blue), 1993-2010 (green), 1999-2010 (orange), and 2005-2010 (pink). Filled bars represent trends that are significant at the 95% significance level. (b) As in (a) but only for the NH (20°N-90°N). (c) As in (a) but for the tropics (20°N-20°S). (d) As in (a) but for the Southern Hemisphere (SH; 20°S-90°S).

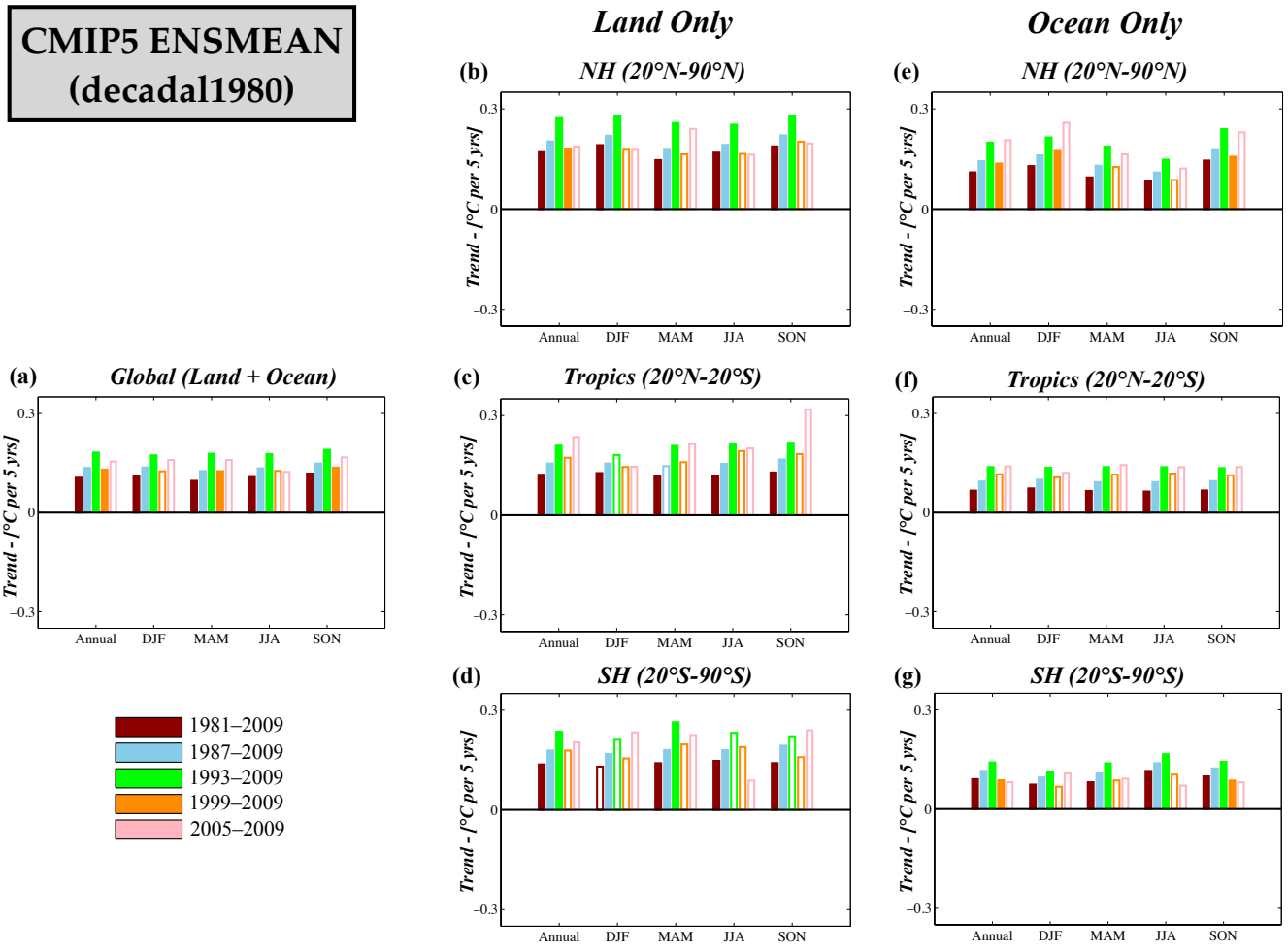

Fig. S2. The linear trend in area-averaged global surface temperature (°C per 5 years) over *land and ocean* from the CMIP5 decadal1980 simulations. Filled bars represent trends that are significant at the 95% significance level. (b)-(d) The linear trend in averaged *land* surface temperature only (°C per 5 years) in the (b) NH (20°N-90°N), (c) the tropics (20°N-20°S), and (d) the SH (20°S-90°S). Filled bars as in (a). (e)-(g) As in (b)-(d) but for *ocean* surface temperatures.

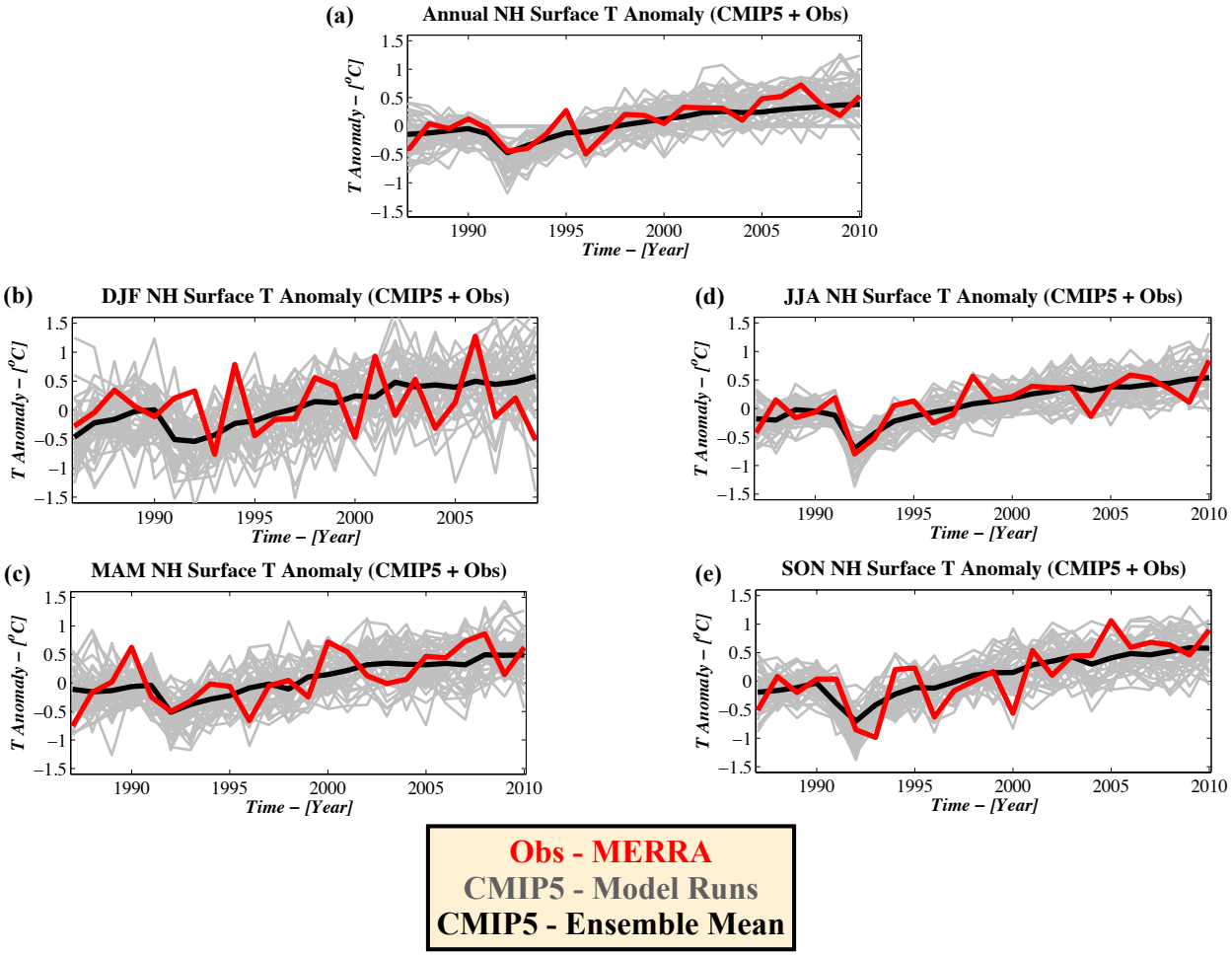

Fig. S3 (a) Annual land surface temperature anomaly (°C), area-averaged poleward of 20°N, from 1987-2010 from NASA MERRA (red), the 42 individual model runs (gray), and the ensemble-mean (black). (b)-(e) As in (a) but for (b) DJF, (c) MAM, (d) JJA, and (e) SON.

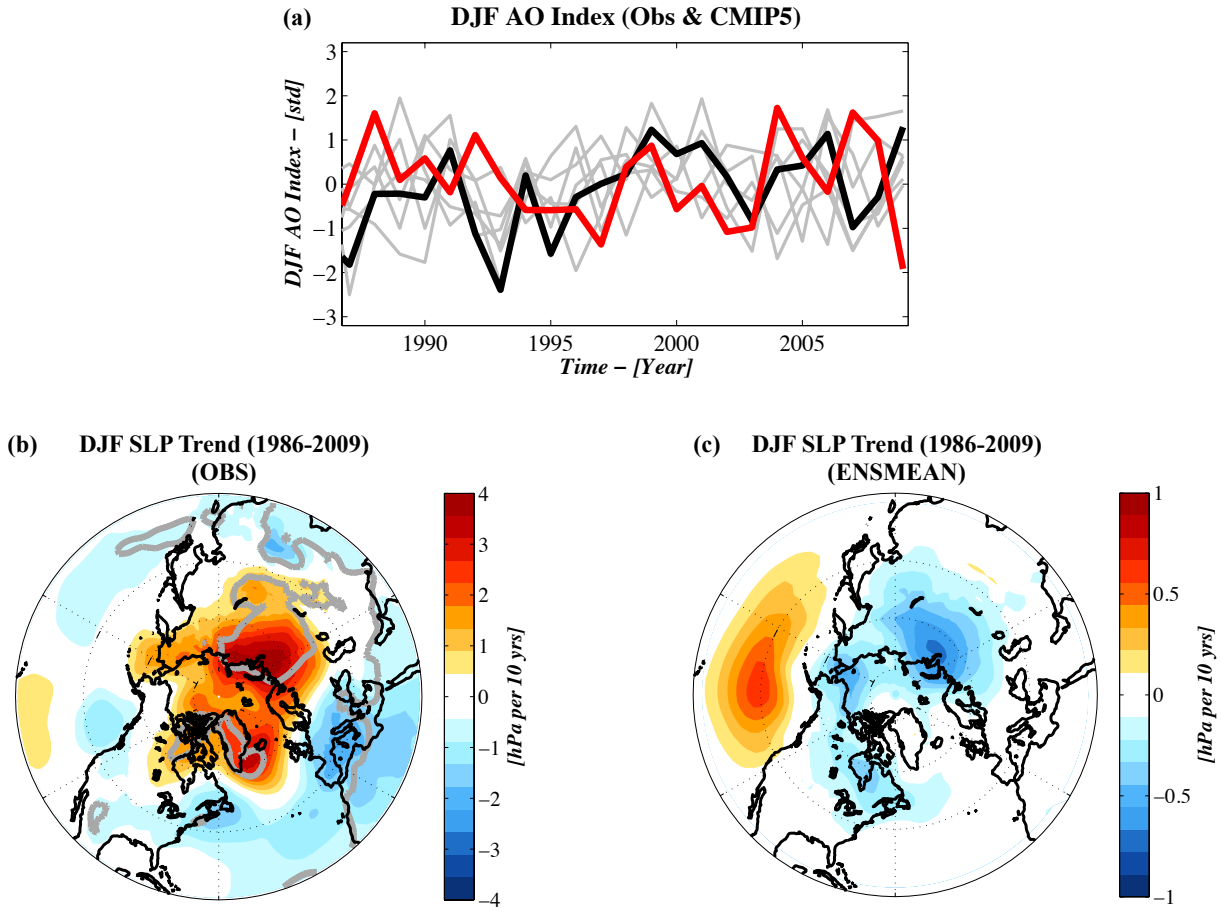

Fig. S4. (a) The standardized DJF average AO index (defined as the difference in sea level pressure between regions between 35-55°N and regions poleward of 65°N) from MERRA (red), the six CMIP5 models (gray), and the ensemble-mean of all models (black) from 1986/87-2009/10. (b) The decadal SLP trend (hPa per 10 years) from MERRA for 1986/87-2009/10. (c) As in (b) but the CMIP5 ensemble-mean decadal trend in SLP. Values that exceed the 95% confidence interval are delineated by gray contour (i.e., none of the values in (c) are significant).